Supporting Information

Wide-Spectral/Dynamic-Range Skin-Compatible Phototransistors Enabled by Floated Heterojunction Structures with Surface Functionalized SWCNTs and Amorphous Oxide Semiconductors

Insik Hwang[1†], Jaehyun Kim[1†], Minkyung Lee[2], Min-Wook Lee[1], Hee-Joong Kim[1], Hyuck-In Kwon[1], Do Kyung Hwang[3], Myunggil Kim[4], Haeyoung Yoon[5], Yong-Hoon Kim[2], and Sung Kyu Park[1]**

[1] School of Electrical and Electronics Engineering, Chung-Ang University, Seoul 06974, Korea

[2] School of Advanced Materials Science and Engineering and SKKU Advanced Institute of Nanotechnology (SAINT), Sungkyunkwan University, Suwon, Korea

[3]Center for Opto-Electronic Materials and Devices, Post-Silicon Semiconductor Institute, Korea Institute of Science and Technology (KIST), Seoul, Korea

[4] Department of Chemistry, Chung-Ang University, Seoul, Korea

[5] Department of Electrical and Computer Engineering, University of Utah, Salt Lake City, UT 84112, U.S.A

†: Equal contribution

*Corresponding Author: Prof. Sung Kyu Park and Porf. Yong-Hoon Kim

Phone: 82-2-820-5347, Fax: 82-2-820-5347,

Email: skpark@cau.ac.kr and yhkim76@skku.edu

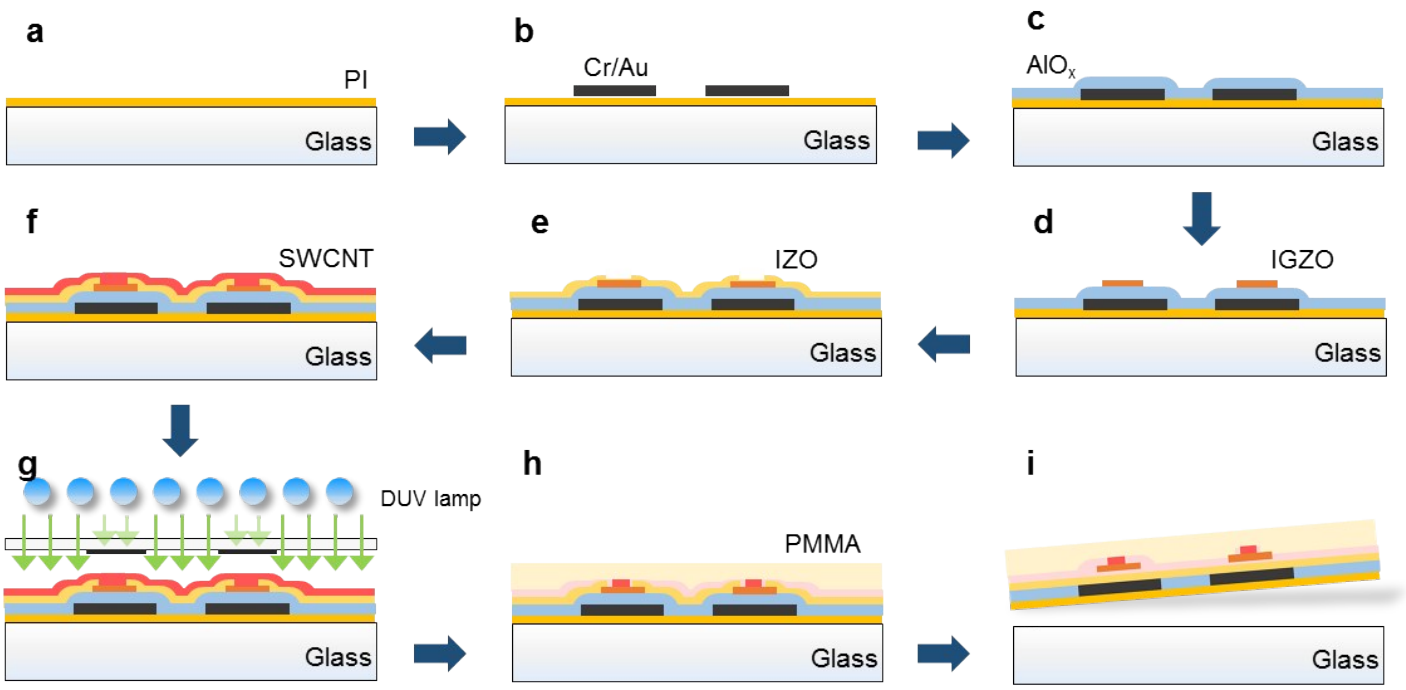

Figure S1. Fabrication process for a sc-SWCNT/a-IGZO heterogeneous phototransistor. a. PI substrate coating. b. Deposition of Cr/Au gate electrode. c. Deposition of Al_2O_3 gate insulator using ALD. d. IGZO precursor solution coating and photochemical activation. e. Deposition of IZO source/drain electrodes. f. sc-SWCNT channel layer coating. g. DUV photochemical patterning of sc-SWCNT layer. h. PMMA passivation. i. Exfoliation of the PI substrate from the carrier glass substrate.

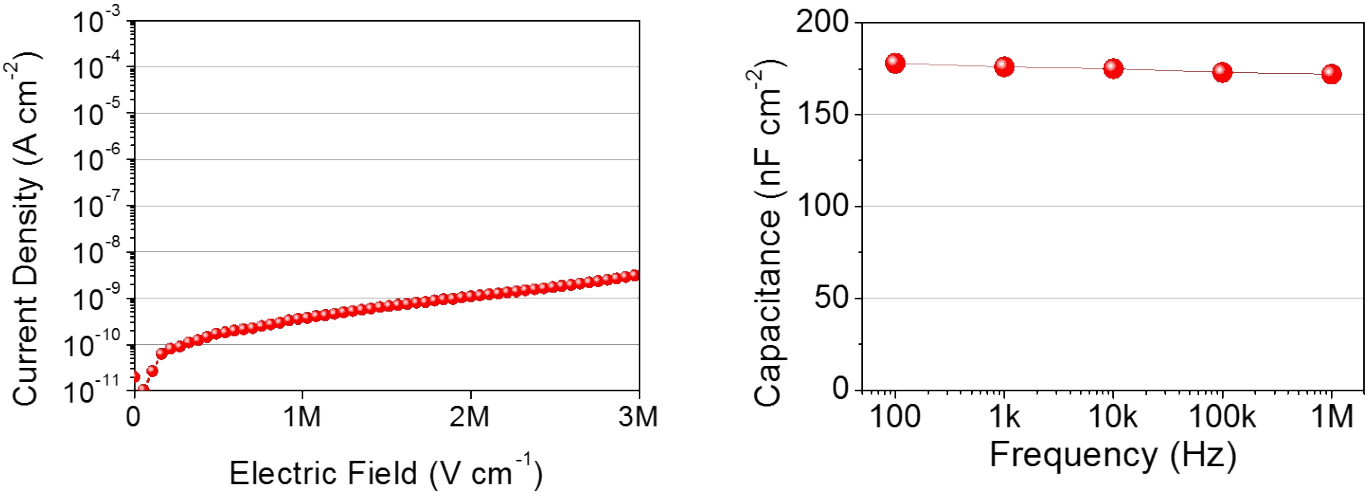

Figure S2. Current density vs. electric field characteristics and areal capacitance vs. frequency characteristics of an Al_2O_3 gate dielectric layer deposited by ALD method.

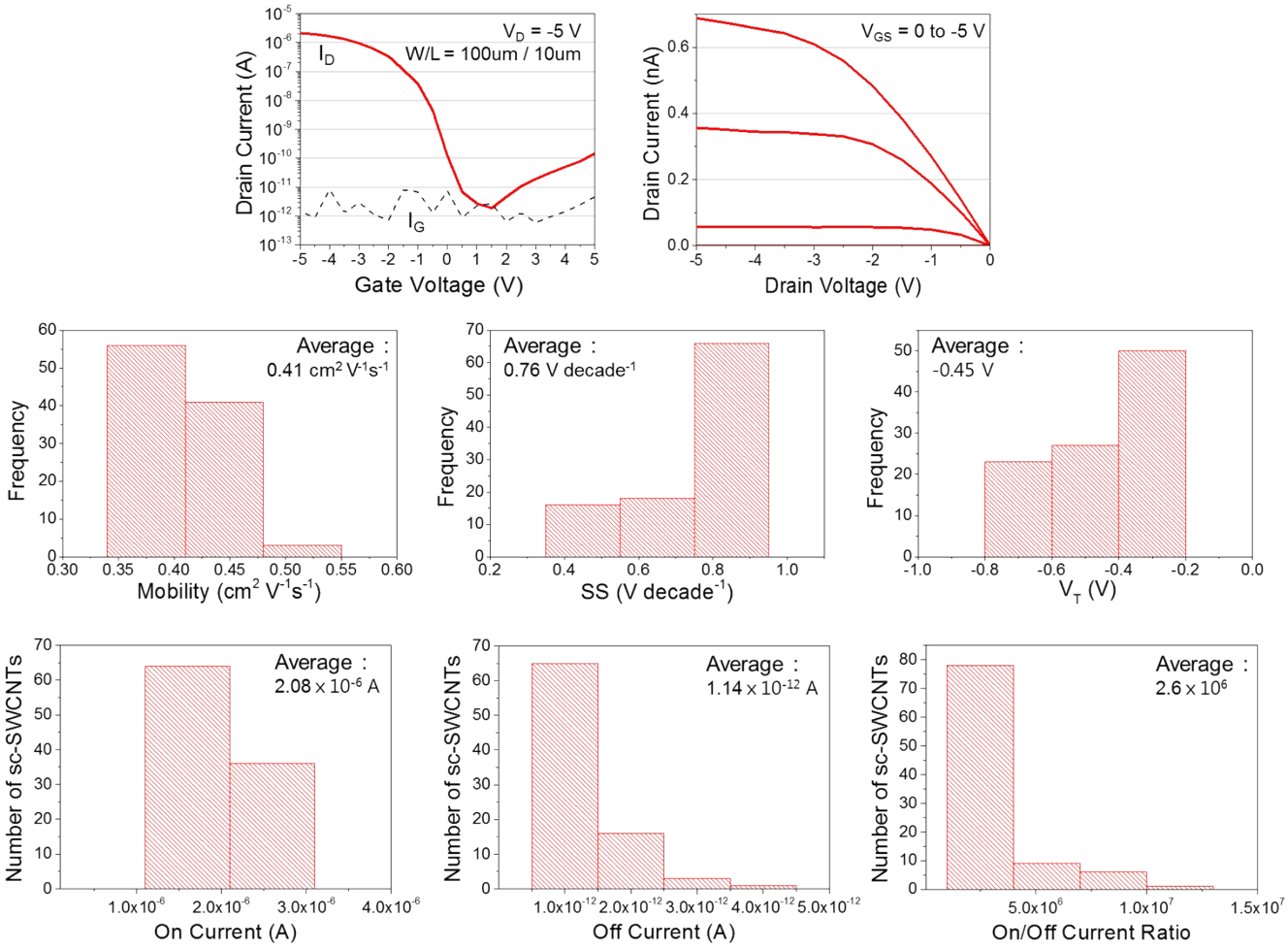

Figure S3. Transfer and output characteristics and statistical data of sc-SWCNT TFTs. The statistical data of field-effect mobility, sub-threshold swing (SS), threshold voltage (V_T), on-current, off-current, and on/off current ratios were obtained from 100 sc-SWCNT TFT devices (V_D = -5 V, W/L = 100 / 50 μm).

ΔV_T (V)	Blue 406 nm	Green 520 nm	Red 638 nm	IR 780 nm
IGZO TFT	3.95	1.62	0.25	0
Hybrid device	9.6	7.07	2.98	1.06

Table S1. Threshold voltage shifts for *a*-IGZO TFT and sc-SWCNT/*a*-IGZO hybrid device in the range of 406 ~ 780 nm wavelength of light.

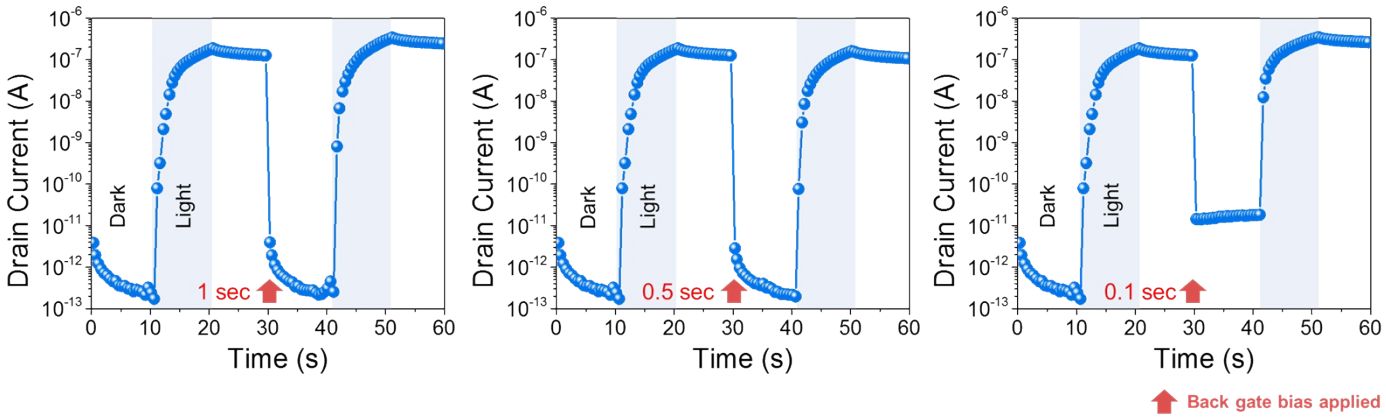

Figure S4. The dynamic photoresponse behavior of sc-SWCNT/*a*-IGZO hybrid phototransistors under a pulsed-light illumination. Here, the V_{DS} was set at 10 V and the V_{GS} was set at -0.5 V. The wavelength of the pulsed-light was 638 nm and light intensity was 3 mW/cm^2. Back gate bias (10 V for 1, 0.5, 0.1 sec) was applied to eliminate PPC effect.

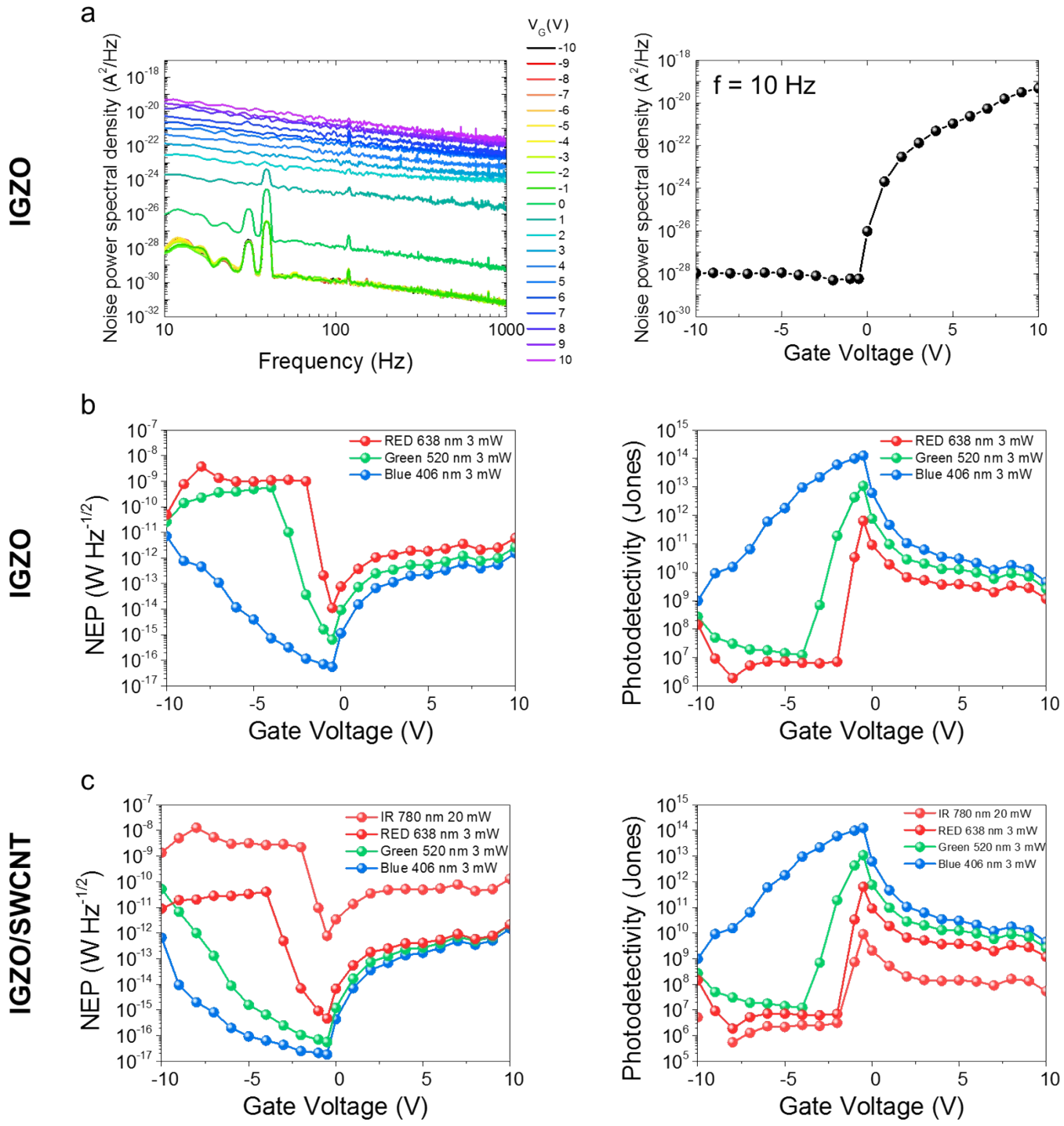

Figure S5. a. Noise power spectral density (S_I), b. noise equivalent power (NEP), and photodetectivity (D^*) of *a*-IGZO TFTs. c. NEP and photodetectivity of sc-SWCNT/*a*-IGZO hybrid devices. The photodetectivity was extracted at V_{DS} = 10 V and V_{GS} = - 0.5 V with light intensity of 3 mW/cm^2 for R/G/B and 20 mW/cm^2 for NIR.

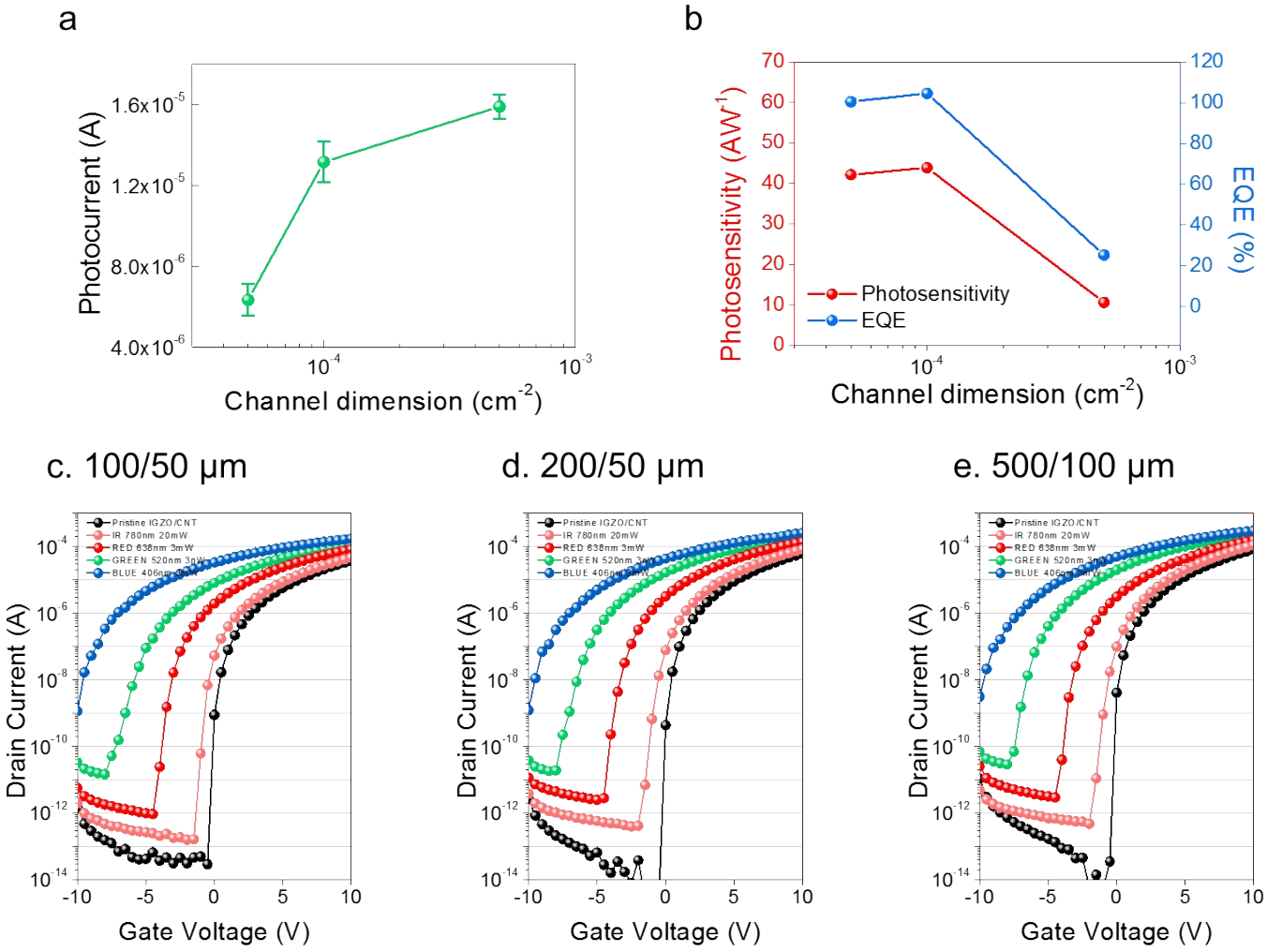

Figure S6. a. Photocurrent, b. photosensivity, external quantum efficiency (EQE), and c~e. photoresponse characteristics of sc-SWCNT/*a*-IGZO hybrid phototransistors with respect to channel width to length ratio. (W/L = 100/50 μm (c), 200/50 μm (d), and 500/100 μm (e), V_{DS} = 10 V, V_{GS} = -0.5 V with light intensity of 3 mW/cm^2 for R/G/B, and 20 mW/cm^2 for NIR.

External quantum efficiency (EQE) was calculated by the definition.

$$EQE = (J_{ph}/q) / (P/hv)$$

where J_{ph} is the photocurrent density, q is the electronic charge, P is light power, and hv is the photon energy.

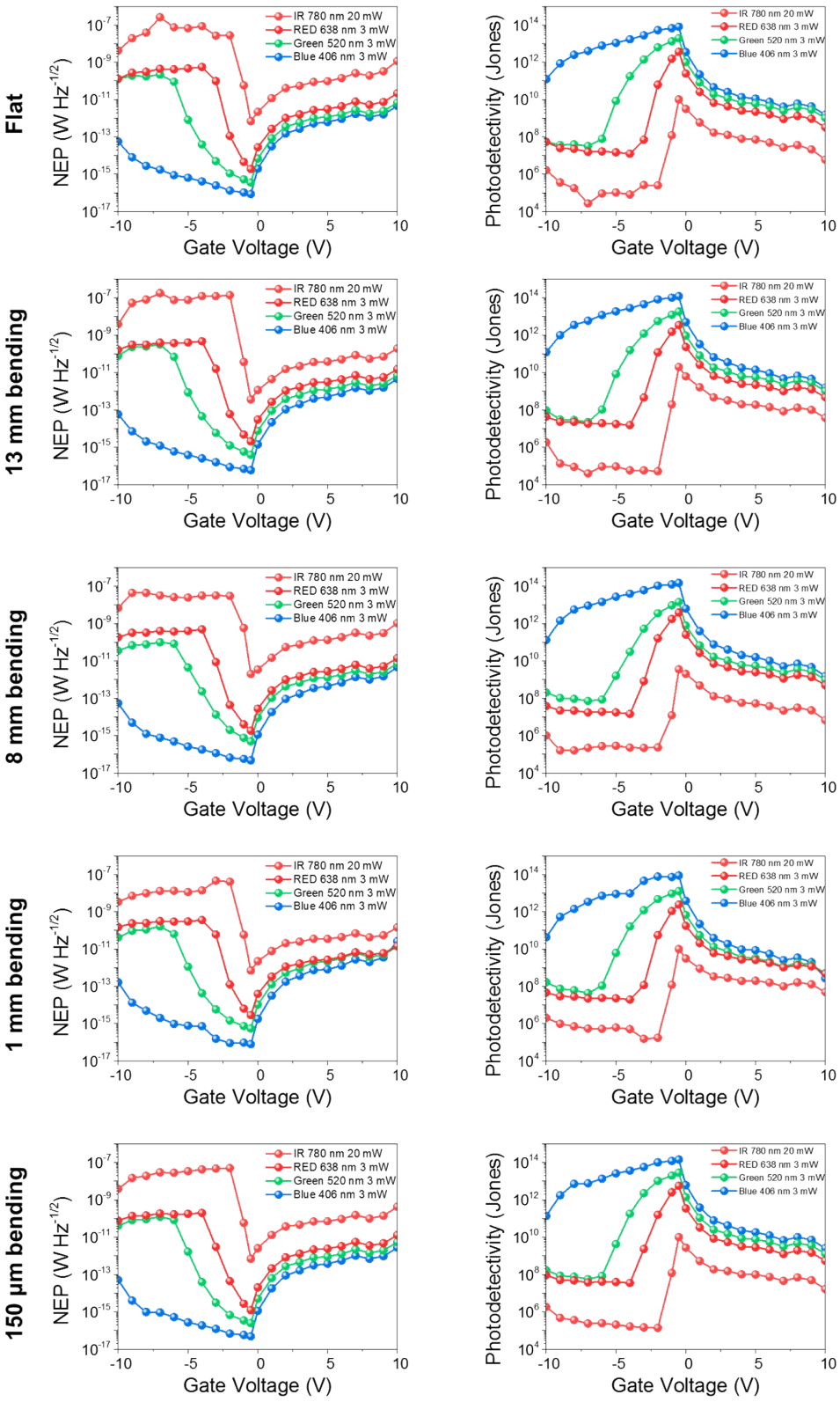

Figure S7. Noise equivalent power (NEP), and photodetectivity (D^*) of ultra-flexible sc-SWCNT/a-IGZO hybrid phototransistors with bent surfaces measurement. Note that hybrid photosensors were kept adhered to the curvatures of 13, 8, 1 mm, and 150 μm during the measurement. The photodetectivity were extracted at V_{DS} = 10 V and V_{GS} = -0.5 V with light intensity of 3 mW/cm^2 for R/G/B, and 20 mW/cm^2 for NIR.

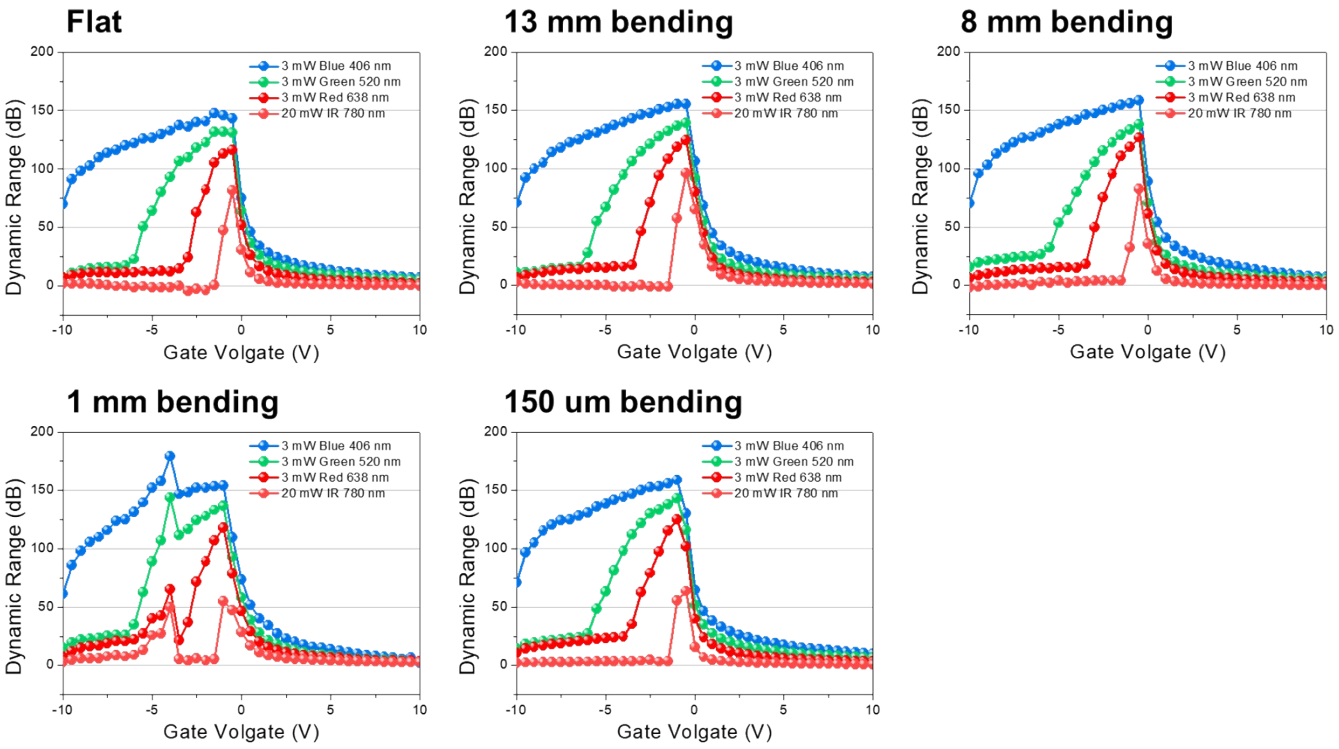

Figure S8. Dynamic range (dB) of ultra-flexible sc-SWCNT/a-IGZO hybrid phototransistors with bent surfaces measurement. Note that hybrid photosensors were kept adhered to the curvatures of 13, 8, 1 mm, and 150 μm during the measurement. The photodetectivity were extracted at V_{DS} = 10 V and V_{GS} = -0.5 V with light intensity of 3 mW/cm^2 for R/G/B, and 20 mW/cm^2 for NIR.

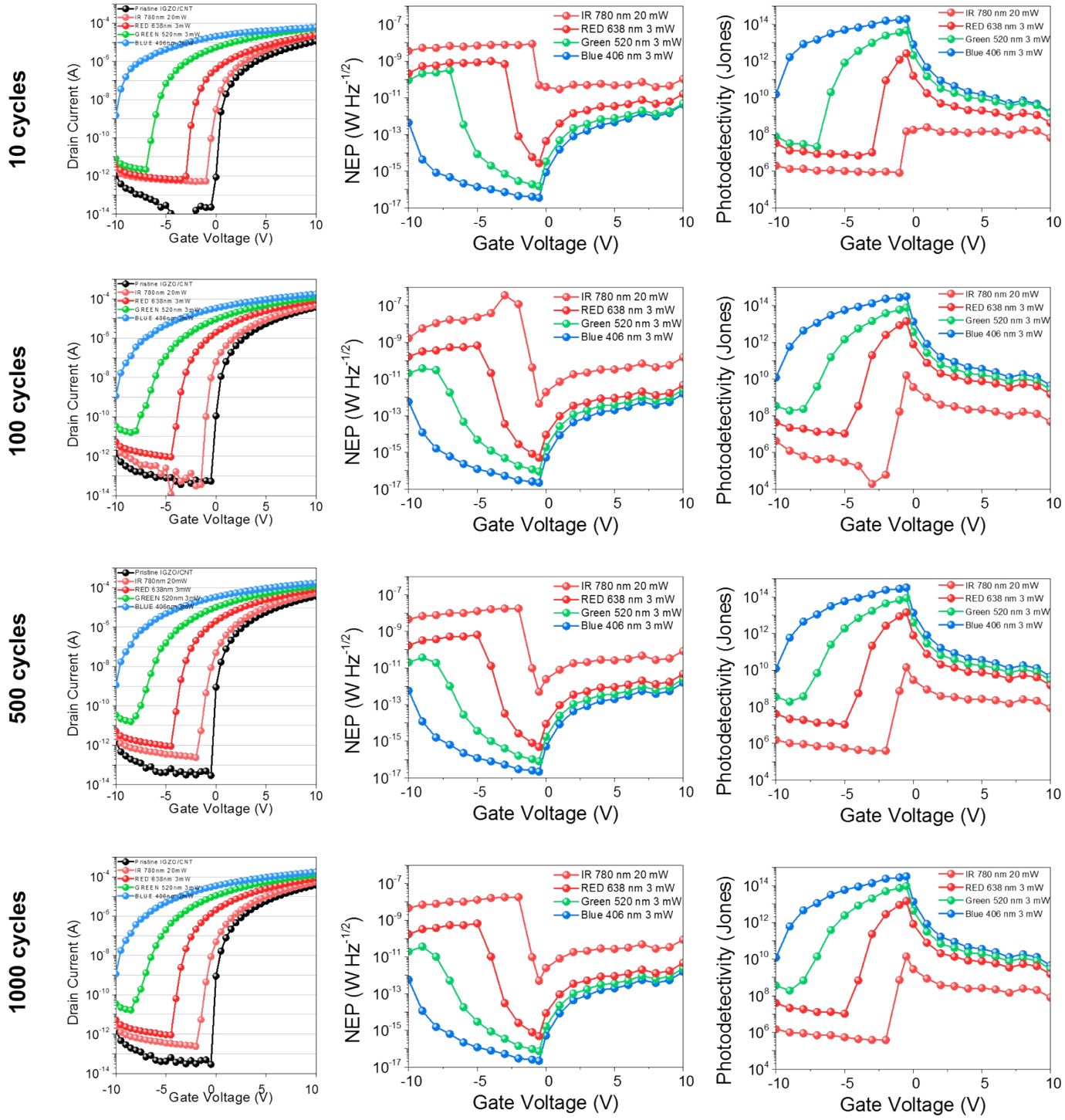

Figure S9. Photoresponse characteristics, noise equivalent power (NEP), and photodetectivity (D^*) of ultra-flexible sc-SWCNT/a-IGZO hybrid phototransistors with respect to cyclic bending test. Bending radius is about 150 μm. The photodetectivity were extracted at V_{DS} = 10 V and V_{GS} = -0.5 V with light intensity of 3 mW/cm^2 for R/G/B, and 20 mW/cm^2 for NIR.

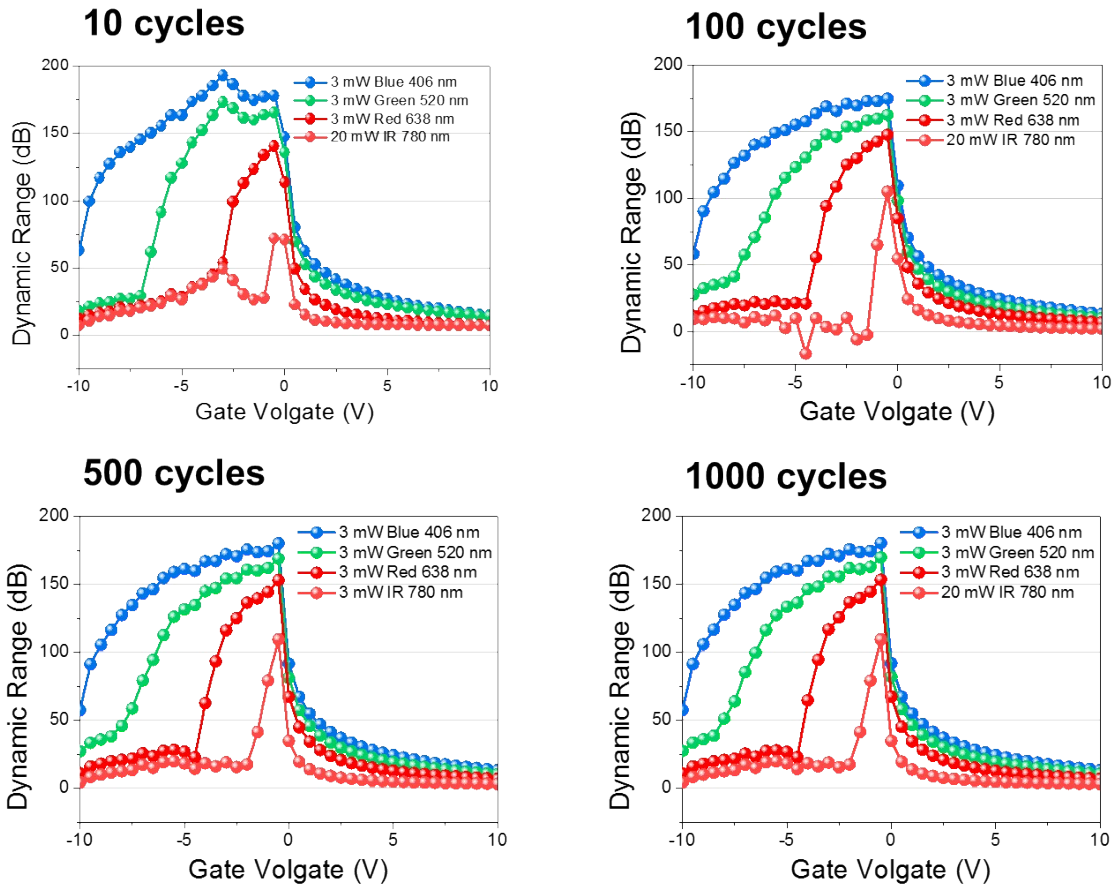

Figure S10. Dynamic range (dB) of ultra-flexible sc-SWCNT/a-IGZO hybrid phototransistors with respect to cyclic bending test. Bending radius is about 150 μm. The photodetectivity were extracted at V_{DS} = 10 V and V_{GS} = -0.5 V with light intensity of 3 mW/cm^2 for R/G/B, and 20 mW/cm^2 for NIR.

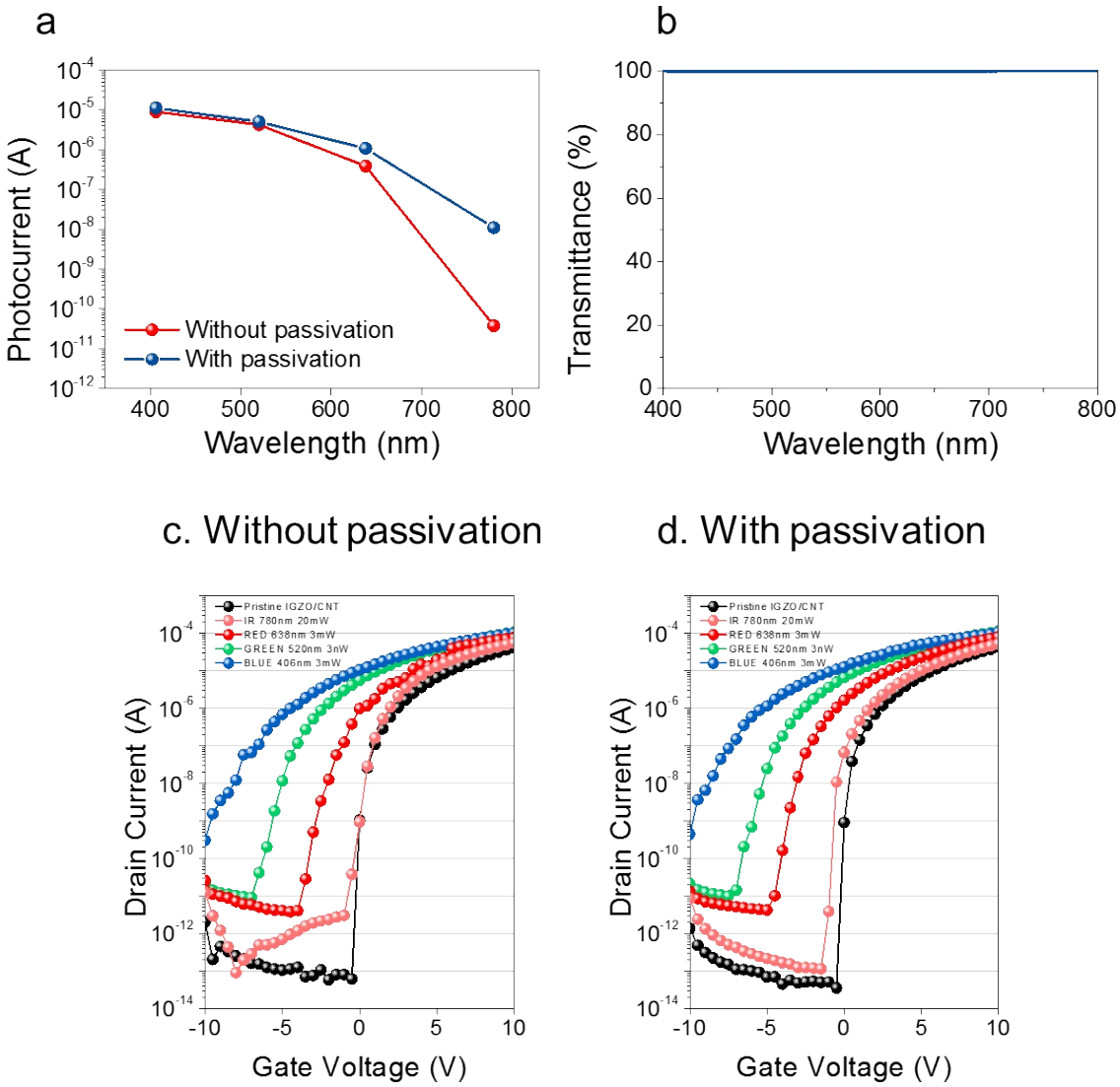

Figure S11. a. Photocurrent behaviors of sc-SWCNT/a-IGZO hybrid phototransistors without/with PMMA passivation, (W/L = 100/50 μm, VDS = 10 V, VGS = -0.5 V with light intensity of 3 mW/cm2 for R/G/B, and 20 mW/cm2 for NIR). b. Optical transmittance of PMMA film, c, d. Photoresponse characteristics of sc-SWCNT/a-IGZO hybrid phototransistors without/with PMMA passivation.